AD_____

Award Number: DAMD17-01-1-0277

TITLE: Recombinational Repair Genes and Breast Cancer Risk

PRINCIPAL INVESTIGATOR: Naoko Shima, Ph.D.

CONTRACTING ORGANIZATION: The Jackson Laboratory
Bar Harbor, Maine 04609-1500

REPORT DATE: July 2004

TYPE OF REPORT: Annual Summary

PREPARED FOR: U.S. Army Medical Research and Materiel Command
Fort Detrick, Maryland 21702-5012

DISTRIBUTION STATEMENT: Approved for Public Release;
Distribution Unlimited

REPORT DOCUMENTATION PAGE

Form Approved
OMB No. 074-0188

1. AGENCY USE ONLY (Leave blank)	2. REPORT DATE	3. REPORT TYPE AND DATES COVERED
	July 2004	Annual Summary (1 Jul 2001 - 30 Jun 2004)

4. TITLE AND SUBTITLE
Recombinational Repair Genes and Breast Cancer Risk

5. FUNDING NUMBERS
DAMD17-01-1-0277

6. AUTHOR(S)
Naoko Shima, Ph.D.

7. PERFORMING ORGANIZATION NAME(S) AND ADDRESS(ES)
The Jackson Laboratory
Bar Harbor, Maine 04609-1500

E-Mail: nshima@jax.org

8. PERFORMING ORGANIZATION REPORT NUMBER

9. SPONSORING / MONITORING AGENCY NAME(S) AND ADDRESS(ES)
U.S. Army Medical Research and Materiel Command
Fort Detrick, Maryland 21702-5012

10. SPONSORING / MONITORING AGENCY REPORT NUMBER

11. SUPPLEMENTARY NOTES

12a. DISTRIBUTION / AVAILABILITY STATEMENT
Approved for Public Release; Distribution Unlimited

12b. DISTRIBUTION CODE

13. ABSTRACT (Maximum 200 Words)

To seek novel DNA double strand break (DSB) repair genes that may influence breast cancer risk, conducted a phenotype-based screen for chromosome instability mutations in mice, successfully yielding four mutations. Underlying genes for two of these mutations have been identified and their effects on carcinogenesis have been investigated.

chaos1 (chromosome aberration occurring spontaneously 1) was the first mutation identified from this screen. This recessive mutation was linked with a missense mutation in *Polq* encoding DNA polymerase θ, which is potentially involved in DNA inter-strand cross-link repair. We confirmed that *chaos1* is a mutant allele of *Polq* using two genetic approaches. Although the *chaos1* allele itself does not confer higher cancer susceptibility, interestingly we observed genetic interaction between *chaos1* and *Atm* (ataxia telangiectasia mutated), which has a central role in regulating DSB repair by homologous recombination, and presumably influences breast cancer susceptibility.

Chaos3 is a semi-dominant mutation associated with a missense mutation in *Mcm4* (Minichromosome maintenance deficient 4 homolog), which is essential for DNA replication in all eukaryotes. The allelism between *Chaos3* and *Mcm4* was genetically confirmed. Most importantly, *Chaos3* homozygous females are highly susceptible to spontaneous mammary tumors, presenting a new mouse model for breast cancer studies.

14. SUBJECT TERMS
No subject terms provided.

15. NUMBER OF PAGES
29

16. PRICE CODE

17. SECURITY CLASSIFICATION OF REPORT	18. SECURITY CLASSIFICATION OF THIS PAGE	19. SECURITY CLASSIFICATION OF ABSTRACT	20. LIMITATION OF ABSTRACT
Unclassified	Unclassified	Unclassified	Unlimited

Table of Contents

Introduction

It was hypothesized in my proposal that DNA double strand break (DSB) repair could be one of the most important factors in breast tumor suppression, considering the functions of BRCA1 and BRCA2 in DSB repair by homologous recombination (1). In addition, enhanced radiosensitivity of lymphocytes from unselected breast cancer patients has been reported (2), further suggesting that defects in DSB repair are associated with increased risk of breast cancer. Fundamental mechanisms for DSB repair seem to be conserved through in eukaryotes (3, 4). However, mammalian genomes are much larger and far more complicated in structure, so additional unknown genes are probably involved, which may influence breast cancer risk. Therefore, I have chosen forward genetics approaches for the identification of such novel genes/alleles in mice to investigate their effects in carcinogenesis in the context of a whole organism.

1. **Screen for dominant mutants in recombinational repair using embryonic stem (ES) cells**
2. **Use of ES cell lines bearing different deletions to screen for recessive mutants**

In Task1 and 2, ES cell mutagenesis and its combination with chromosome deletion complexes were proposed as one of the screen methods. However, we are still developing this technology. More importantly, the experiments described in Task3 went extremely well, and I decided to focus on them.

3. **Screen for radiation-sensitive mutants in whole animals using a micronucleus test**

3.1 Summary of the micronucleus screen

Defects in DSB repair could confer hypersensitivity to ionizing radiation as well as elevated incidences of spontaneous chromosome aberrations (i.e. chromosome instability). To induce mutations that potentially cause such phenotypes, C57BL/6J males were mutagenized with the powerful germline mutagen *N*-ethyl-*N*-nitrosourea (5, 6) and were bred in a classical three-

generation cross scheme to produce their descendants that can be possibly homozygous for induced recessive mutations. To screen mutant mice for radiation hypersensitivity and chromosome instability, I have adapted the flow cytometric peripheral blood micronucleus assay to quantitate chromosome damage *in vivo* (7, 8). Micronuclei arise from acentric chromosome fragments or whole chromosomes that have not been incorporated in the main nuclei at cell division (9), thus representing chromosome breaks and aneuploidy. For the enumeration of micronuclei, erythrocytes are particularly suitable, because they expel their nuclei, but not micronuclei, after their last mitotic division. We have recovered at least four mutations among 763 pedigrees derived from the mutagenized males. A detailed description of the micronucleus screen can be found in Appendix 1.

3.2. *chaos1*

3.2.1. *chaos1* is a mutant allele of *Polq*

chaos1 (chromosome aberration occurring spontaneously 1) is the first mutation identified in this screen. Treatment with radiation or mitomycin C (MMC) induced significantly higher frequencies of micronuclei in *chaos1/chaos1* mice to a level that indicates hypersensitivity to agents inducing DSB or inter-strand cross-links. This recessive mutation was genetically mapped on a 1.3 Mb interval on Chromosome 16 (10). Among the genes residing in this region was *Polq* encoding DNA polymerase θ (theta). POLQ is homologous to Drosophila MUS308 that is believed to be involved in DNA inter-strand cross-link repair (11-13). Its orthologs do not exist in single cellular organisms such as bacteria and yeast. POLQ is also unique in that it contains both a helicase domain near the N-terminus and a polymerase domain in the C-terminal end (10, 12, 14). Mutation analysis of *Polq* cDNA coding sequence revealed that *chaos1/choas1* mice contain a T to C transition creating Ser1932Pro change, which is not present in the parental strain C57BL/6J (10). However, since this is not located in a conserved or critical region, it was thus uncertain whether or not this missense mutation actually compromises gene function. Therefore, we confirmed that *chaos1* is a mutant allele of *Polq* by two complementary approaches. First, expression of wild-type *Polq* from a bacterial artificial chromosome (BAC) clone (RP24-108G13) corrected

the *chaos1* mutant phenotype (Fig. 1). Second, a *Polq* disrupted allele (*Polq*$^{-}$) generated by gene-targeting failed to complement *chaos1* (Fig. 2). Therefore, the *chaos1* allele will be termed as *Polq*^{m1chaos1Jcs} (*Polq*^{chaos1}) hereafter. However, it remains to be elucidated how the missense mutation Ser1932Pro compromises or abolishes POLQ biochemical function(s).

To determine whether *Polq*$^{-/-}$ mice have a phenotype different from *Polq*^{chaos1} mutants, *Polq*$^{-/-}$ mice were produced by intercrossing heterozygotes. Among 11 litters genotyped, homozygotes for the disrupted allele (*Polq*$^{-/-}$) were born at expected Mendelian ratios (data not shown). The homozygotes appear normal through 8 months of age as do *Polq*^{chaos1}/*Polq*^{chaos1} mice. Micronucleus frequencies of *Polq*$^{-/-}$mice were essentially indistinguishable from *Polq*^{chaos1} homozygotes.

3.2.2. Potential role of *Polq* in carcinogenesis

Polq^{chaos1}/*Polq*^{chaos1} mice were monitored for development of malignancies until 17 months of age, however, they were not prone to any spontaneous tumors. Therefore, the *Polq*^{chaos1} mutation was placed in a sensitized background to investigate its potential role in carcinogenesis.

Ataxia telangiectasia (A-T) is human cancer syndrome due to germline mutation in ATM (ataxia telangiectasia mutated), which has a central role in double strand break (DSB) recognition and signaling of the repair pathway (15). A-T patients exhibit pleiotropic symptoms: hypersensitivity to ionizing radiation, neurodegeneration, immunodeficiency, sterility, and higher susceptibility to lymphoid malignancies. Interestingly, certain types of *ATM* mutations have been linked with increased risk of breast cancer (16).

To characterize genetic interaction between *Polq* and *Atm* and potential involvement of *Polq* in lymphomagenesis, we bred the *Polq*^{chaos1} mutation under an *Atm* deficiency (17). As previously reported, the number of double mutants was much less than expected by Mendelian ratios and thus the combination of these two mutations is partially lethal (data not shown). It was determined that double mutant died within a few days after birth by timed-mating experiments (data not shown). Surviving double mutants are severely growth retarded and show increased genome instability (Fig. 3), although they have a much longer

latency for thymic lymphoma than the *Atm*$^{-/-}$ mice (Fig. 3). It was recently reported that *POLQ* expression was upregulated in a wide range of human cancers accompanied with poor clinical outcome (18). Considering a potential role of *POLQ* in cross-link repair, it is possible that higher *POLQ* expression could confer increased resistance to anti-cancer drugs, many of which are cross-linkers. Future studies using the mutant *Polq* mice presented here including the BAC transgenic mice will explore these possibilities.

3.3. *Chaos3*

3.3.1. *Chaos3* mutant mice carry a mutation in *Mcm4*

Chaos3 is a semi-dominant mutation that confers distinctive phenotypes in heterozygotes and homozygotes. While *Chaos3* heterozygotes show only a mild increase in spontaneous micronucleus levels, the homozygotes exhibit astonishingly higher levels of spontaneous micronuclei, a 20-fold increase over wild-type mice (Fig. 4). However, *Chaos3* mutant mice do not exhibit radiation sensitivity, as do *chaos1/chaos1* mice. By positional cloning, we mapped *Chaos3* to an interval on Chromosome 16 that contains *Mcm4* (Minichromosome maintenance deficient 4 homolog). Mutation analysis revealed a single T to A base substitution in the coding region of *Mcm4* in *Chaos3* carriers. This mutation creates an amino acid change from Phe345Ile in the highly conserved MCM domain (Fig. 4).

To gain further evidence, we carried out a complementation test between *Chaos3* and a known *Mcm4* mutant allele. BayGenomics offers mutant mouse embryonic stem (ES) cell clones created by insertional mutagenesis using gene-trap vectors (19). The gene-trap vectors were designed to express truncated mRNA of a mutated gene, which is tagged with the marker *β-geo* (a fusion gene of *β-gal* and *neo*), when the insertion occurs in an intron of a gene. These insertional events could potentially abolishe or interfere with the gene function, creating a null or hypomorphic allele. Therefore, we searched the BayGenomics database, identifying two *Mcm4* mutant ES cell clones. We obtained one of these clones (RRE056) to generate *Mcm4* mutant mice. To verify that clone RRE056 indeed carries a *Mcm4* mutation, I performed reverse-transcriptase polymerase chain reaction (RT-PCR) on RNA isolated from clone RRE056 to confirm the

expression of the fusion mRNA of *Mcm4* and *β-geo*. Resulting cDNA product was sequenced to identify the junction between *Mcm4* and *β-geo* sequences (Fig. 5). Furthermore, PCR on genomic DNA revealed the exact insertion site (Fig. 5). These data localized the insertion site in the intron between exons 12 and 13 of *Mcm4*. Since these exons correspond to a part of the highly conserved MCM domain, this insertion most likely creates a null allele of *Mcm4* (*Mcm4*$^{-}$). Indeed, *Mcm4*$^{-/-}$ mice were never recovered from intercrosses between *Mcm4*$^{-}$ carriers among 25 offspring genotyped, as those observed in lower eukaryotes (20). A male *Mcm4*$^{-}$ heterozygote was then mated with a *Chaos3* homozygous female for the complementation test. Among 10 offspring genotyped, no *Mcm4*$^{-}$ carriers were recovered, failing to rescue the lethality of *Mcm4*$^{-}$ allele. These data confirm the allelism between *Chaos3* and *Mcm4*

3.3.2 *Chaos3* homozygotes are highly susceptible to malignancies

MCM proteins are a family of six conserved proteins that are essential for eukaryotic DNA replication (20). MCM proteins interact with each other to form the hexameric MCM complex, a component of the pre-replication complex that plays a crucial role in origin licensing (20). It has been also suggested that a sub-complex of MCM proteins might serve as the replicative helicase during elongation of replication forks (21). Therefore, MCM proteins contribute to maintaining genomic integrity through ensuring successful DNA replication. Nevertheless, potential effects of germline mutations in *Mcm* genes in genome maintenance/cancer have not been investigated in mammals. This is probably due to the fact that complete disruption of essential *Mcm* genes by gene targeting would result in lethality. However, homozygotes at the hypomorphic mutation *Chaos3* are viable and most remarkably 50% of the homozygous females succumb to mammary tumors at age 10-14 months. Lymphoma is the second most frequently observed malignancy in both males and females. A large-scale cohort study is currently ongoing to confirm these results and to obtain more detailed profiles of these tumors.

These data provide a new paradigm indicating a connection between DNA replication defects and cancer. To our knowledge, this is the first demonstration of a *Mcm* gene as a tumor suppressor gene in mice, suggesting

potential involvement of *MCM* genes in human hereditary and spontaneous cancers.

4. Investigation of effects of meiosis-specific DMC1 on mitotic recombination

We are still seeking a suitable system, which ensures stable expression of *Dmc1* in somatic cells.

Key Research Accomplishments

- Transgene rescue and complementation test with a *Polq* null allele created by gene-targeting confirmed that *chaos1* is a mutant allele of *Polq*.
- *chaos1* exhibits genetic interaction with *Atm*, a gene that potentially influences breast cancer risk.
- *Chaos3* is a hypomorphic mutation in *Mcm4*, which has essential roles for DNA replication in all eukaryotes.
- *Chaos3* homozygotes are highly prone to spontaneous tumors, particularly to mammary adenocarcinomas.
- Two more mutations have been also recovered and await further analysis.

Reportable outcomes

Presentation

Shima N, Hartford SA, Duffy T, Wilson LA, Schimenti KJ, Schimenti JC
New mutations causing chromosome instability in mice, Radiation Research Society meeting, April 2004, St. Louise, Missouri

Shima N, Hartford SA, Duffy T, Wilson LA, Schimenti KJ, Schimenti JC
Two chromosome instability mutants identified by mouse ENU mutagenesis screen, Gordon Research Conference, Mammalian DNA repair, January 2003, Ventura, California

Shima N, Hartford SA, Duffy T, Wilson LA, Schimenti KJ, Schimenti JC

Identification of chromosome instability mutants by a flow cytometric mouse peripheral blood micronucleus assay, Mouse initiatives III, August 2001, The Jackson Laboratory

Publications

Shima N, Hartford SA, Munroe RJ, Mikaelian I, Wilson LA, Schimenti JC (2004) *Chaos3* encodes a novel hypomorph mutation in murine *Mcm4*, which confers chromosome instability and higher susceptibility to spontaneous malignancies. in preparation.

Shima N, Munroe, RJ, Schimenti JC (2004) The mouse genomic instability mutation *chaos1* is an allele of *Polq* that exhibits genetic interaction with *Atm*. Submitted to Molecular Cellular Biology.

Shima N, Hartford SA, Duffy T, Wilson LA, Schimenti KJ, Schimenti JC (2003) Phenotype-based identification of mouse chromosome instability mutants. Genetics 163: 1031-1040

Conclusions

The micronucleus screen has yielded novel mutations such as *chaos1* and *Chaos3*. Underlying genes for these two mutations were identified and their effects on carcinogenesis were investigated. *chaos1* has been proven as a mutant of a novel DNA repair gene *Polq*, which shows genetic interaction with *Atm*, a key player in DSB repair and tumor suppression. It was also confirmed that *Chaos3* is a hypomorphic allele of *Mcm4*. *Chaos3* homozygotes succumb to spontaneous tumors (particularly mammary tumors) within the first year of life. Additionally, we have recovered two more chromosome instability mutations, which await further analysis. With this screen, it is possible to identify a variety of alleles in involved in diverse pathways of DNA metabolism, as long as they exhibit elevated levels of spontaneous micronuclei.

References

1. A. R. Venkitaraman, *Cell* **108,** 171 (2002).
2. D. Scott, J. B. Barber, A. R. Spreadborough, W. Burrill, S. A. Roberts, *Int J Radiat Biol* **75,** 1 (1999).
3. P. Karran, *Curr Opin Genet Dev* **10,** 144 (2000).
4. R. Kanaar, J. H. Hoeijmakers, D. C. van Gent, *Trends Cell Biol.* **8,** 483 (1998).
5. S. Hitotsumachi, D. A. Carpenter, W. L. Russell, *Proc Natl Acad Sci U S A* **82,** 6619 (1985).
6. R. Balling, *Annu Rev Genomics Hum Genet* **2,** 463 (2001).
7. J. A. Heddle, *Mutat Res* **18,** 187 (1973).
8. T. Morita, *et al, Mutat Res* **389,** 3 (1997).
9. M. Nusse, B. M. Miller, S. Viaggi, J. Grawe, *Mutagenesis* **11,** 405 (1996).
10. N. Shima, S. A. Hartford, T. Duffy, L. A. Wilson, K. J. Schimenti, J. C. Schimenti, *Genetics* **163,** 1031 (2003).
11. J. B. Boyd, K. Sakaguchi, P. V. Harris, *Genetics* **125,** 813 (1990).
12. P. V. Harris, O. M. Mazina, E. A. Leonhardt, R. B. Case, J. B. Boyd, K. C. Burtis, *Mol Cell Biol* **16,** 5764(1996).
13. E. A. Leonhardt, D. S. Henderson, J. E. Rinehart, J. B. Boyd, *Genetics* **133,** 87 (1993).
14. M. Seki, F. Marini, R. D. Wood, *Nucleic Acids Res* **31,** 6117 (2003).
15. M. S. Meyn, *Clin Genet* **55,** 289 (1999).
16. R. A. Gatti, A. Tward, P. Concannon, *Mol Genet Metab* **68,** 419 (1999).
17. C. Barlow, *et al., Cell* **86,** 159 (1996).
18. K. Kawamura, *et al., Int J Cancer* **109,** 9 (2004).
19. D. Stryke, *et al., Nucleic Acids Res* **31,** 278 (2003).
20. B. K. Tye, *Annu Rev Biochem* **68,** 649 (1999).
21. K. Labib, T. A. Tercero, J. F.Diffley, *Science* **288,** 1643 (2000).

Figure Legend

Fig. 1. Phenotype rescue by BAC transgene. (A) BAC transgenic founder females (generated in B6 background) were outcrossed to C3H.B6-*chaos1*/*chaos1* males (N10F1) in which the *chaos1* allele had been introduced into C3H genome by backcrossing nine generations. This was necessary to identify Chromosome 16 that carries the *chaos1* allele. Resulting F1 males carrying the BAC transgene were mated with C3H.B6-*chaos1*/*chaos1* females. Among the offspring, *chaos1*/*chaos1* mice were identified as those homozygous for the C3H alleles of the two polymorphic microsatellite markers *D16Mit131* (proximal) and *D16Mit106* (distal). *chaos1*/*chaos1* mice were phenotyped by the micronucleus assay. The transgene (Tg) carriers exhibited a normal range of spontaneous micronucleus frequency, indicating the phenotype correction by the transgene. (B) Spontaneous micronucleus frequencies were measured in CD71-negative normochromatic erythrocytes (NCE; lower quadrants of the plots). Micronucleated erythrocytes (MN-NCE) are in the population positive to propidium iodide (lower right quadrant). Anti-CD71 antibody was used to separate reticulocytes (younger erythrocytes) containing significant amounts of RNA, which potentially interferes with accurate enumeration of micronuclei in NCE. The transgene carriers show a normal range of micronucleus frequencies as comparable to those seen in wild-type mice, while *chaos1*/*chaos1* mice exhibited significantly higher micronucleus frequencies, indicating complete phenotype correction. At least 10,000 erythrocytes were collected.

Fig. 2. *Polq* gene targeting strategy. (A) Schematic representation of a part of the genomic *Polq* locus. The first six exons are indicated as boxes with numbers.

Locations of selected restriction sites are shown. (B) The targeting construct was designed to replace exons 2-5 with a neomycin resistance gene (neo) by homologous recombination. Filled rectangles represent genomic sequences used for each arm, one of which contains a part of exon 1 modified to contain a premature stop codon (TGA). The position of the negatively selectable marker thymidine kinase (tk) is also shown. Small arrows indicate the direction of transcription. (C) The disrupted allele lacks exons 2-5 and contains modified exon1 with a stop codon just after the initiation codon. (D) Southern blot analysis of correctly targeted ES cell clones, in which the expected sizes of *Bam*HI (left) and *Eco*RI (right) fragments were detected by the probes indicated in "C." (E) Representative flow plots of micronucleus assays on *chaos1*/*Polq*$^{-}$ mice and *Polq*$^{-/-}$ mice. Spontaneous micronuclei in CD71-negative normochromatic erythrocytes were detected by propidium iodide.

Fig. 3.Synergistic phenotypes observed in *Atm*/*Polq*^{chaos1} double homozygotes. (A) Growth curves of mice of male (left) and female (right) with indicated genotypes. Each point represents at least five animals and is shown with standard deviation. (B) Enhanced spontaneous micronucleus formation in *Atm*/*Polq*^{chaos1} double homozygotes. Micronuclei in CD71-negative erythrocytes were detected by propidium iodide. (C) The *Polq*^{chaos1} mutation significantly delays development of thymic lymphoma in *Atm* deficient mice (p<0.0005, t-test). (D) Cell growth of MEFs. *Atm*/*Polq*^{chaos1} double homozygous cell show severely impaired proliferation. Each point is shown with standard deviation. Experiments were replicated at least once using two independent MEF lines.

Fig. 4. *Chaos3* mutant phenotypes and associated missense mutation found in *Mcm4*. (A) Representative flow plots of the micronucleus assay. Spontaneous micronuclei in CD71-negative normochromatic erythrocytes were detected by propidium iodide. Whereas *Chaos3* heterozygotes (left) exhibit a mild increase in spontaneous micronucleus levels over wild-type (middle), the homozygotes show a 20-fold increase (right), indicative of enhanced chromosome instability. (B) Phe345Ile mutation found in *Chaos3* mutant mice. MCM4 protein contains 862 amino acids. Conserved domains such as MCM and ATPase are indicated with corresponding amino acid numbers. The identified mutation is located in a position carboxyl to the zing finger motif, which has important roles in DNA binding and interaction with other MCM members.

Fig. 5. Clone RRE056 carries an insertional mutation in *Mcm4*. Sequence traces indicate (A) the presence of a fusion cDNA of *Mcm4* and *β-geo* recovered from clone RRE056 by RT-PCR and (B) genomic sequence of the insertion site, which is localized in *Mcm4* intron 12. VectorpGT01xf sequence was identified after 16 ambiguous bases in intron 12 of *Mcm4*.

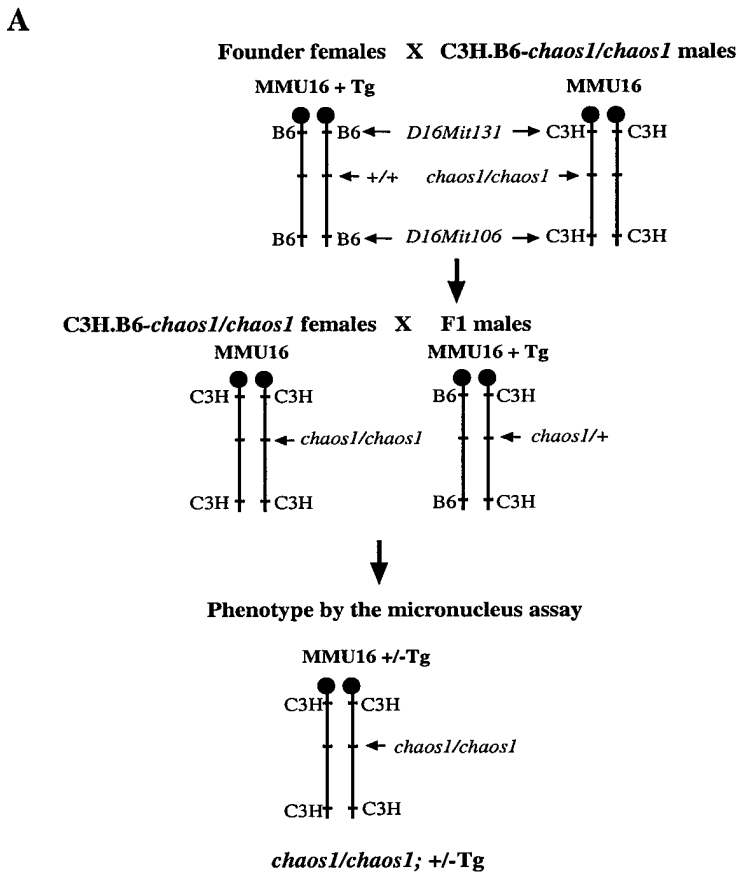
A
Founder females X C3H.B6-chaos1/chaos1 males
MMU16 + Tg
MMU16
B6
B6
D16Mit131
C3H
C3H
+/+
chaos1/chaos1
B6
B6
D16Mit106
C3H
C3H
C3H.B6-chaos1/chaos1 females X F1 males
MMU16
MMU16 + Tg
C3H
C3H
chaos1/chaos1
B6
C3H
chaos1/+
C3H
C3H
B6
C3H
Phenotype by the micronucleus assay
MMU16 +/-Tg
C3H
C3H
chaos1/chaos1
C3H
C3H
chaos1/chaos1; +/-Tg

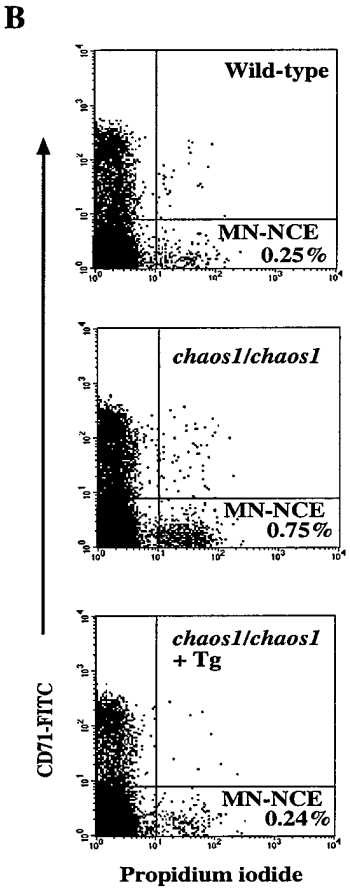
B
Wild-type
MN-NCE
0.25%
chaos1/chaos1
MN-NCE
0.75%
chaos1/chaos1
+ Tg
MN-NCE
0.24%
CD71-FITC
Propidium iodide

Fig. 1

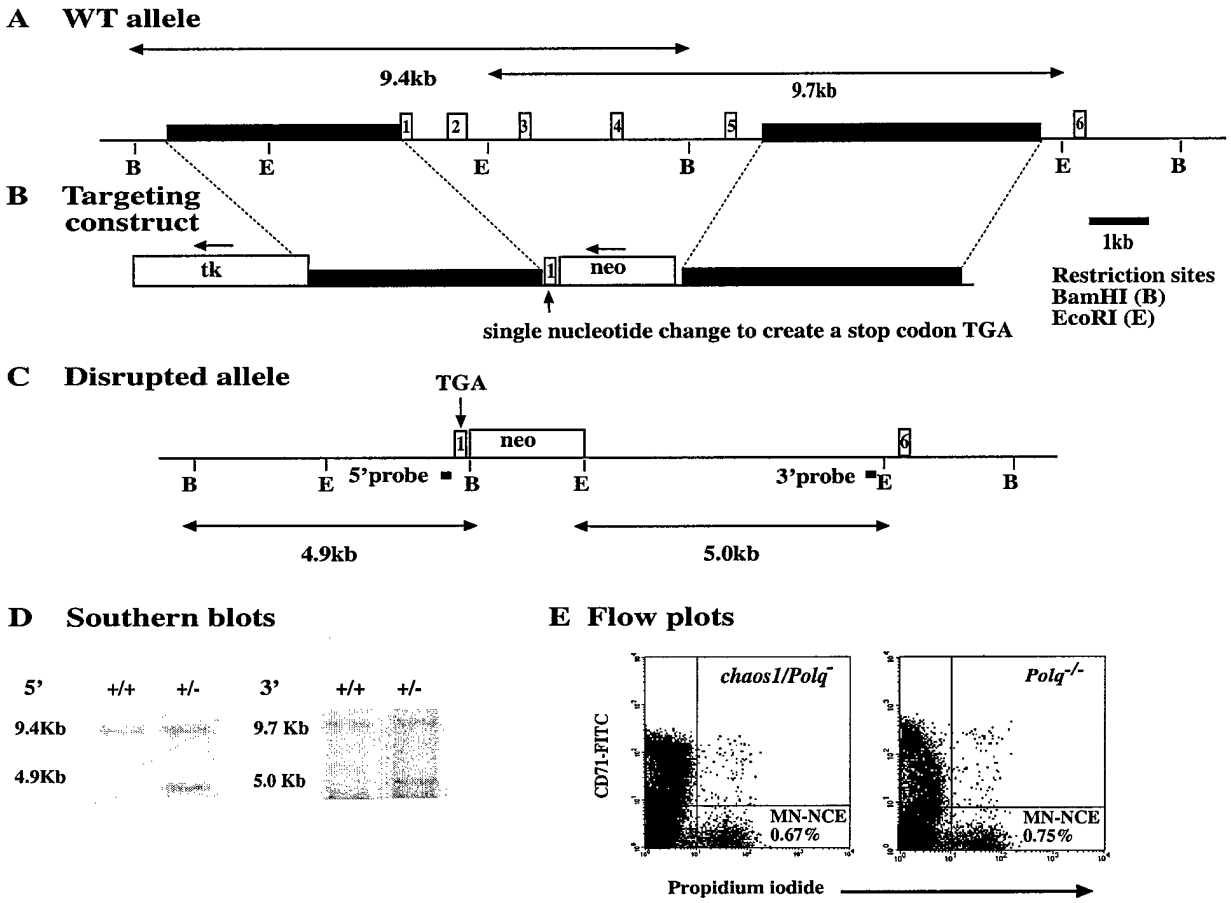
A WT allele
9.4kb
9.7kb
1
2
3
4
5
6
B
E
E
B
E
B
B Targeting construct
tk
1
neo
1kb
Restriction sites
BamHI (B)
EcoRI (E)
single nucleotide change to create a stop codon TGA
C Disrupted allele
TGA
1
neo
6
B
E
5'probe
B
E
3'probe
E
B
4.9kb
5.0kb
D Southern blots
5'
+/+
+/-
3'
+/+
+/-
9.4Kb
4.9Kb
9.7 Kb
5.0 Kb
E Flow plots
chaos1/Polq-
Polq-/-
CD71-FITC
MN-NCE
0.67%
MN-NCE
0.75%
Propidium iodide

Fig. 2

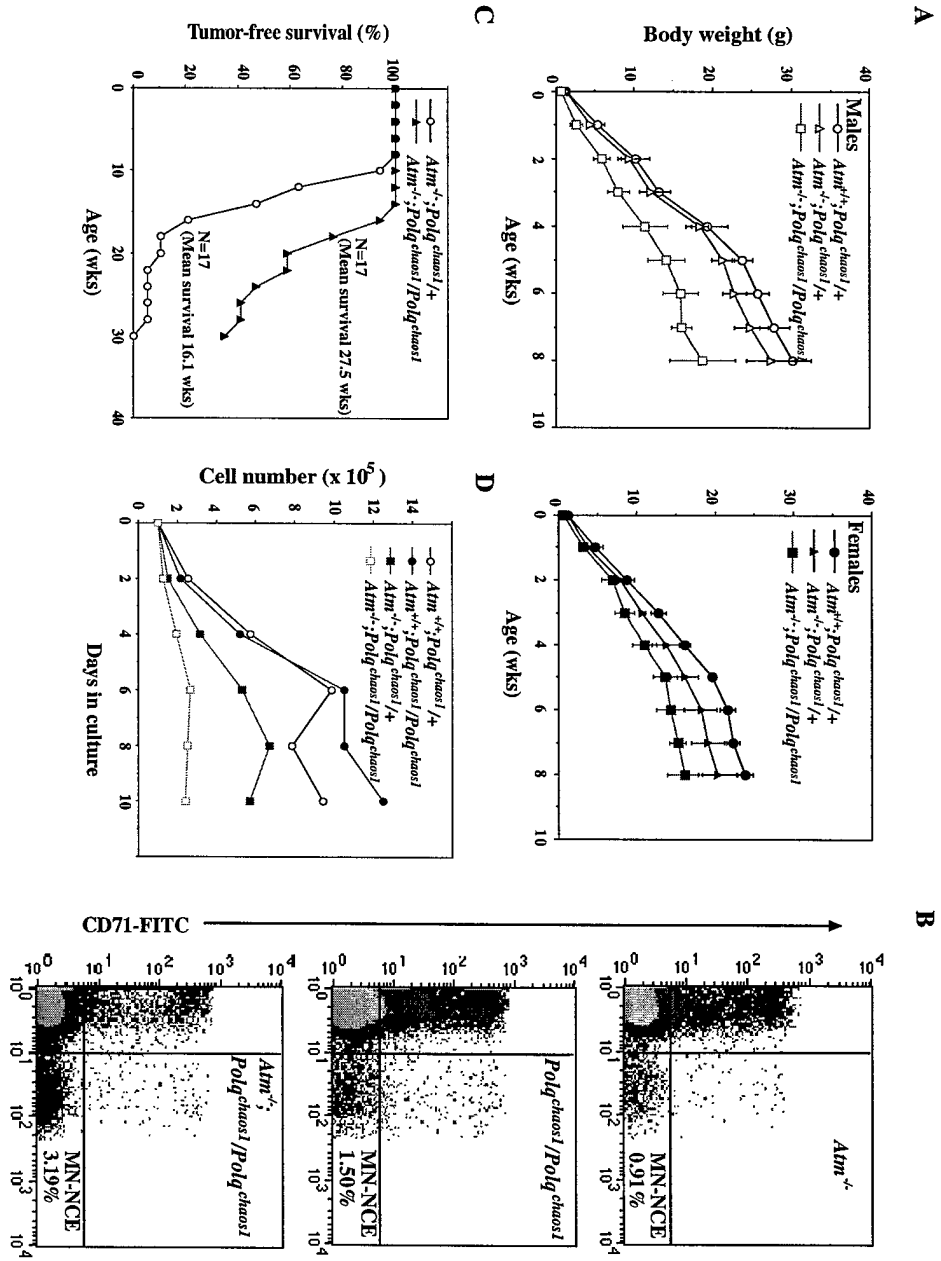
A
Body weight (g)
Age (wks)
Males
Atm+/+;Polq chaos1/+
Atm-/-;Polq chaos1/+
Atm-/-;Polq chaos1/Polq chaos1
Females
Atm+/+;Polq chaos1/+
Atm-/-;Polq chaos1/+
Atm-/-;Polq chaos1/Polq chaos1
B
CD71-FITC
propidium iodide
Atm-/-
MN-NCE 0.91%
Polq chaos1/Polq chaos1
MN-NCE 1.50%
Atm-/-; Polq chaos1/Polq chaos1
MN-NCE 3.19%
C
Tumor-free survival (%)
Age (wks)
Atm-/-;Polq chaos1/+
Atm-/-;Polq chaos1/Polq chaos1
N=17 (Mean survival 16.1 wks)
N=17 (Mean survival 27.5 wks)
D
Cell number (x 10^5)
Days in culture
Atm +/+;Polq chaos1/+
Atm+/+;Polq chaos1/Polq chaos1
Atm-/-;Polq chaos1/+
Atm-/-;Polq chaos1/Polq chaos1

Fig. 3

A

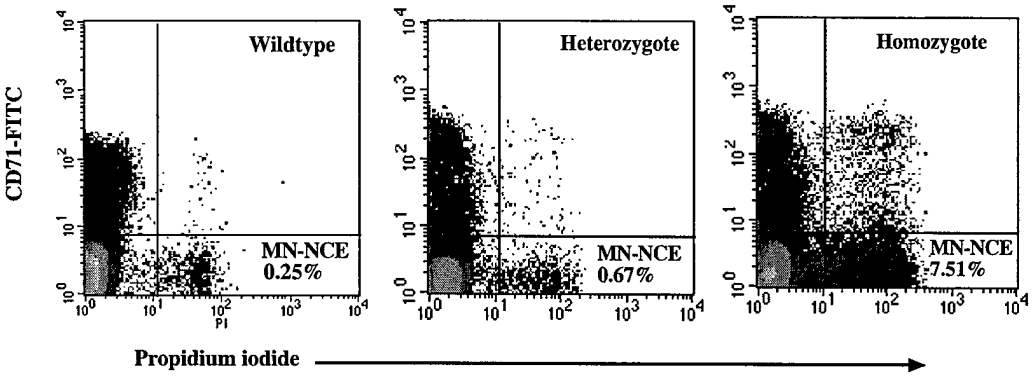
CD71-FITC
Wildtype
MN-NCE
0.25%
Heterozygote
MN-NCE
0.67%
Homozygote
MN-NCE
7.51%
PI
Propidium iodide

B

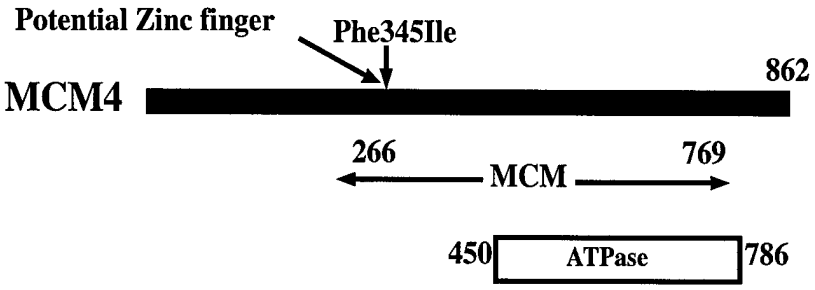
Potential Zinc finger
Phe345Ile
MCM4
862
266
MCM
769
450
ATPase
786

Fig. 4

A. RT-PCR

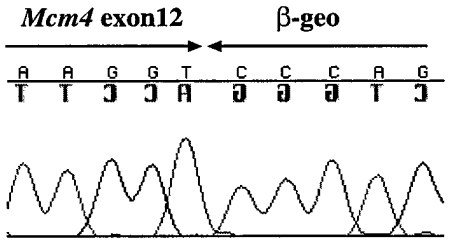

B. Genomic PCR

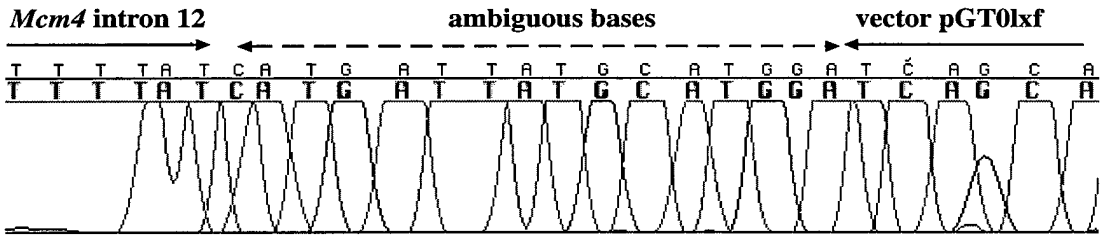

Fig. 5

Phenotype-Based Identification of Mouse Chromosome Instability Mutants

Naoko Shima, Suzanne A. Hartford, Ted Duffy, Lawriston A. Wilson, Kerry J. Schimenti and John C. Schimenti[1]

The Jackson Laboratory, Bar Harbor, Maine 04609

Manuscript received September 13, 2002
Accepted for publication November 20, 2002

ABSTRACT

There is increasing evidence that defects in DNA double-strand-break (DSB) repair can cause chromosome instability, which may result in cancer. To identify novel DSB repair genes in mice, we performed a phenotype-driven mutagenesis screen for chromosome instability mutants using a flow cytometric peripheral blood micronucleus assay. Micronucleus levels were used as a quantitative indicator of chromosome damage *in vivo*. Among offspring derived from males mutagenized with the germline mutagen *N*-ethyl-*N*-nitrosourea (ENU), we identified a recessive mutation conferring elevated levels of spontaneous and radiation- or mitomycin C-induced micronuclei. This mutation, named *chaos1* (*ch*romosome *a*berration *o*ccurring *s*pontaneously *1*), was genetically mapped to a 1.3-Mb interval on chromosome 16 containing *Polq*, encoding DNA polymerase θ. We identified a nonconservative mutation in the ENU-derived allele, making it a strong candidate for *chaos1*. POLQ is homologous to Drosophila MUS308, which is essential for normal DNA interstrand crosslink repair and is unique in that it contains both a helicase and a DNA polymerase domain. While cancer susceptibility of *chaos1* mutant mice is still under investigation, these data provide a practical paradigm for using a forward genetic approach to discover new potential cancer susceptibility genes using the surrogate biomarker of chromosome instability as a screen.

CHROMOSOME instability is a hallmark of cancer cells. It may arise from defects in chromosome metabolism, including DNA double-strand-break (DSB) repair. DSBs can lead to chromosome aberrations and to mitotic recombination, either of which can result in loss of heterozygosity. As seen in individuals with certain cancer syndromes, DSB repair defects may cause chromosome instability, increasing cancer risk. For example, ataxia telangiectasia and the Nijmegen breakage syndrome (DIGWEED *et al.* 1999; MEYN 1999) are attributed to germline mutations in genes regulating DSB repair signaling. Werner, Bloom, and Rothmund-Thomson syndromes (VAN BRABANT *et al.* 2000) are all caused by mutations in RecQ-like genes, which are thought to be involved in repair of DSBs by homologous recombination (HR). Furthermore, the breast cancer susceptibility genes *BRCA1* and *BRCA2* also function in DSB repair, particularly in the regulation of HR (VENKITARAMAN 2002). Inactivation of these genes also causes genomic instability (SHEN *et al.* 1998; TUTT *et al.* 1999; KRAAKMAN-VAN DER ZWET *et al.* 2002). In sum, DSB repair appears to have an important role in genome maintenance and tumor suppression. To achieve a full understanding of DSB repair and its association with cancer, it is necessary to identify all the genes involved.

Many mammalian genes involved in DSB repair, particularly by HR, have been identified on the basis of homology to those of the yeast *Saccharomyces cerevisiae*, indicating their conserved role in genome maintenance (THACKER 1999). However, it is likely that additional mammalian DSB repair genes do not exist in yeast. For example, there are no yeast homologs of *BRCA1*, *BRCA2*, or *PRKDC* (protein kinase, DNA-activated, catalytic polypeptide). Furthermore, mammals have a larger RAD51 family consisting of seven members with nonredundant function (THOMPSON and SCHILD 2001; VAN GENT *et al.* 2001). Most notably, yeast and mammalian cells have clear differences in the way they repair DSBs. There are two major pathways in DSB repair in mammalian cells, HR and nonhomologous end joining (NHEJ; KARRAN 2000; KHANNA and JACKSON 2001; VAN GENT *et al.* 2001). NHEJ is used heavily in mammalian cells, whereas in yeast, DSBs are repaired almost exclusively by HR (THOMPSON and SCHILD 1999). The NHEJ pathway, which is also involved in V(D)J recombination, joins broken chromosomal ends with little homology and thus is error prone. In the HR repair pathway, a sister chromatid or homologous chromosome is used as a repair template, resulting in higher fidelity. This pathway may be more important during development, since inactivation of most of HR genes results in early embryonic lethality (THOMPSON and SCHILD 2001). It has been suggested that activities of the two DSB repair pathways may be regulated during the cell cycle in mammals (HENDRICKSON 1997; THOMPSON and SCHILD 1999, 2001).

Sequence data from this article have been deposited with the EMBL/GenBank Data Libraries under accession nos. AY074936, AY147862, AY147863, and AY147864.

[1]*Corresponding author:* The Jackson Laboratory, 600 Main St., Bar Harbor, ME 04609. E-mail: jcs@jax.org

DSB repair mutants have been traditionally isolated on the basis of radiation hypersensitivity in yeast and rodent cell lines (THOMPSON *et al.* 1982; JONES *et al.* 1987, 1988; FRIEDBERG *et al.* 1995). At least 11 complementation groups of X-ray-sensitive rodent cell line mutation have been identified (ZDZIENICKA 1999). Eventually, the *in vivo* consequences of mutations in some of these genes were investigated by the generation of gene-targeted mice. Since most of these mutations are recessive, it has been suggested that the mutant identification depended on aneuploidy and/or presence of hemizygous loci in these cell lines (JONES *et al.* 1988). Thus it is possible that many genes were undetectable by such screens.

Forward genetic mutation screens in mice offer several advantages for the identification of new DSB repair genes. Random *N*-ethyl-*N*-nitrosourea (ENU) mutagenesis of the mouse genome is now a well-established method to isolate both dominant and recessive mutations with high efficiency (JUSTICE *et al.* 1999; HRABE DE ANGELIS *et al.* 2000), and positional cloning of these mutations has been vastly simplified by the availability of mouse genomic sequence and various other genetic resources. If an efficient assay were available to detect chromosome instability, it could be exploited in forward genetic mutation screens to identify novel genes required for DSB repair and/or chromosome stability in mice. Moreover, potential cancer susceptibility can be addressed directly in the mutant mice.

To detect mouse DSB repair mutants, we explored the efficacy of a high-throughput micronucleus assay, which provides a quantitative measure of *in vivo* chromosome damage (HEDDLE 1973). Micronuclei (MN) can arise from acentric chromosome fragments or whole chromosomes that have not been incorporated in the main nuclei at cell division (NUSSE *et al.* 1996). The formation of micronuclei can be stimulated by DNA-damaging agents that induce chromosome breaks or abnormal chromosome segregation, and thus the micronucleus assay has been used as a genetic toxicology tool for quantitative analysis of *in vivo* chromosome damage induced by potential mutagens (MORITA *et al.* 1997). A peripheral blood micronucleus assay has been semiautomated by flow cytometry (DERTINGER *et al.* 1996), making it practical for screening large numbers of mice with high statistical power. We show that this assay has the ability to detect spontaneous and radiation-induced chromosome instability in DSB repair-deficient homozygous *Atm* (ataxia telangiectasia-mutated) and *Prkdc*^{scid} (severe combined immune deficiency) mutant mice.

Here we report a small-scale ENU mutagenesis screen for chromosome instability mutants that yielded three mutations and one potential mutation causing higher spontaneous micronucleus levels. One of the recovered mutations also confers higher radiation-induced micronucleus levels. This newly identified mutation was named *chaos1* (*ch*romosome *a*berration *o*ccurring *s*pontaneously *1*) and mapped to a 1.3-Mb region of chromosome 16 that does not contain any genes known to cause chromosome instability in humans or mice. However, we identified a mutation in *Polq*, an ortholog of Drosophila *mus308*, that resides in this region. Flies mutant at this locus exhibit genome instability and hypermutability in response to certain chemical agents (LEONHARDT *et al.* 1993). These experiments demonstrate the robustness of the flow cytometric micronucleus assay as a high-throughput screening tool to detect mutations causing genome instability and potential cancer susceptibility.

MATERIALS AND METHODS

ENU mutagenesis: ENU preparation and the injection protocol was based on described protocols (JUSTICE 1999). Male C57BL6/J (B6) mice were intraperitoneally injected with 80 mg ENU/kg body weight (Sigma, St. Louis) once a week for 3 weeks at 8–10 weeks of age. They were mated to C3HeB/FeJ (C3H) females to obtain first generation (G_1) sons. The G_1 males were mated to C3H females to obtain second generation (G_2) daughters. In the whole-genome screens, up to four G_2 daughters were backcrossed to their G_1 fathers to generate third-generation (G_3) offspring who were potentially homozygous for mutations transmitted by the G_1. Micronucleus assays were performed on male G_3 progeny.

Some of the animals screened were derived from a region-specific mutagenesis program focused on the ~30-cM region on proximal chromosome 5 spanned by the rump white (*Rw*) inversion. Mutagenized B6 mice were crossed to C3H-*Rw*/+ females, and resulting G_1 males inheriting *Rw* (*Rw*/+*, where the asterisk represents the mutagenized chromosome 5) were crossed to *Rw/Hm* females (*Hm* refers to hammertoe, a semidominant mutation causing webbing of the digits) to yield *Rw*/+* G_2 offspring. Unlike the previous cross where G_2's were crossed to the G_1 father, in this case the G_2's were intercrossed to produce the G_3 generation. Since *Rw* contains a recessive lethal, only *Rw*/+* and +*/+* G_3 offspring were produced. Only 1 +*/+* G_3 male per family was screened by the micronucleus assay. Note that, as a result of the intercross of the G_2's, the non-chromosome 5 mutations could be rendered homozygous, but the proportion of these compared to the former screen is half (G_2 animals carry half the mutational load of a G_1).

Irradiation of mice and flow cytometric micronucleus assay: Six-week-old G_3 males were exposed to 0.7 Gy of γ-rays from a ^{137}Cs source. Forty-eight hours later, 50 μl of peripheral blood was collected from the retro-orbital sinus into a tube containing 250 μl of anticoagulant solution (500 USP heparin/ml saline, Sigma). A total of 180 μl was transferred to a polypropylene centrifuge tube containing 2 ml methanol at −80°. The tubes were struck sharply several times to break up aggregates and then stored at least overnight before further processing. Flow cytometric analysis was performed on a FACScan cytometer (Becton-Dickinson, San Jose, CA) as described (DERTINGER *et al.* 1996). At least 10,000 reticulocytes and 500,000 normochromatic erythrocytes were analyzed per blood sample.

Microscopic scoring of micronuclei: A method using acridine orange (Sigma)-coated slides (HAYASHI *et al.* 1990) was used to score micronuclei under a fluorescent microscope. Five thousand reticulocytes per sample were analyzed for the presence of micronuclei.

SCID phenotyping: A total of 100 μl peripheral blood in

anticoagulant solution was added to 1 ml fluorescence-activated cell sorter (FACS) buffer (Ca/Mg free PBS, 5 mM EDTA, 0.02% NaN_3), mixed, and set on ice. Four milliliters of Gey's buffer (HBSS, 650 mM NH_4Cl, 27 mM glucose) was added to the mixture and placed for 5 min on ice. Cells were pelleted at 500 × *g* for 5 min at 10°. The pellet was washed twice with 4 ml Gey's buffer and once with 4 ml FACS buffer and then resuspended. Fc receptors were blocked for 30 min on ice with a cocktail of anti-CD16/32 (FcγII/II Rc, produced in house) and Rat IgG (Sigma) using 10 μg of each per blood sample. They were then stained with 145-2C11 (hamster anti-mouse CD3ε) phycoerythrin (PE) to label any T-lymphocytes and with anti-mouse Ig κ, light chain FITC (PharMingen, San Diego) for B-lymphocytes. All antibodies were pretitrated for optimal concentration. Staining occurred on ice for 30 min, after which cells were washed with 2 ml FACS buffer, pelleted, and resuspended in 250 μl FACS buffer. A total of 10 μl propidium iodide solution (20 μg/ml in FACS buffer) was added prior to running samples on the FACScan for live/dead cell discrimination.

Polymerase chain reaction (PCR) analysis of microsatellite markers: Genomic DNA was prepared from the tails as described elsewhere (TRUETT *et al.* 2000). Three microliters of genomic DNA was amplified in a total reaction volume of 30 μl under standard PCR conditions. PCR products were analyzed on 3.75% MetaPhor gels (BMA, Rockland, ME).

Reverse transcription-PCR analysis of *Polq* cDNA: Total RNA was extracted from testes using the RNeasy midi kit (QIAGEN, Valencia, CA). Five micrograms of total RNA were used for RT reactions with Super-ScriptII (GIBCO BRL, Rockville, MD) followed by PCR using *Polq* primer pairs. The primer sequences are available upon request. Rapid amplification of cDNA ends (RACE) was conducted with the 5′ RACE system kit and 3′ RACE adapter primer (GIBCO BRL). cDNA was sequenced on an ABI 3700 DNA analyzer (Applied Biosystems, Foster City, CA).

RESULTS

High-throughput assay for detecting chromosome instability in mice: Phenotype-driven mutagenesis is a powerful way to identify new genes and their biological roles in the context of a whole organism. In seeking a high-throughput assay suitable for identifying mutations causing elevated levels of chromosome damage *in vivo*, a highly sensitive and reproducible flow cytometric peripheral blood micronucleus assay (DERTINGER *et al.* 1996) was evaluated.

In peripheral blood, micronuclei can be enumerated clearly in erythrocytes, which expel their nuclei, but not micronuclei, after their last mitotic division. To facilitate the formation of micronuclei, mice were exposed to 0.7 Gy γ-rays from a ^{137}Cs source. In a control experiment, blood was analyzed from a wild-type mouse before and 48 hr after irradiation. In erythrocytes, normochromatic erythrocytes (NCEs) and reticulocytes (RETs) can be distinguished with an anti-CD71 antibody (SERKE and HUHN 1992), and micronuclei are stainable with the nucleic acid binding agent propidium iodide. The frequency of reticulocytes with micronuclei (MN-RETs) increased from 0.29 to 2.6% at 48 hr after γ-irradiation (Figure 1). Induced micronuclei would be observed in RETs, because micronucleus formation requires a mitosis and RETs in the peripheral blood are products of the most recent mitotic cycle. On the other hand, because NCEs lacked nuclei at the time of irradiation, the frequency of MN-NCEs remained relatively constant before and after irradiation; these micronuclei are of spontaneous origin. Therefore, both spontaneous and radiation-induced micronucleus levels could be measured simultaneously in the same sample.

The data obtained by flow cytometry were compared to those obtained by microscopic manual scoring of the same samples. A high correlation ($r^2 = 0.96$) was achieved, demonstrating that the flow cytometric scoring accurately reflects classical micronucleus scoring.

Elevated incidence of micronuclei in DSB-repair-deficient mice: To test the sensitivity and efficacy of the assay in detecting genomic instability/DSB repair mutants, we used two types of radiation-sensitive mice, 129S6/SvEvTac-*Atm*^{tm1Awb} (*Atm*$^{-/-}$) and NOD.CB17-*prkdc*^{scid}/J (NOD scid). As shown in Figure 2, these mutants had significantly higher micronucleus frequencies at 48 hr after irradiation than did controls ($P < 0.0005$ for both *Atm*$^{-/-}$ and NOD scid using the two-tailed *t*-test). In contrast to the SCID mice, the percentage of MN-RETs in *Atm*$^{-/-}$ mice prior to irradiation was significantly higher ($P < 0.0001$) than that in controls, indicating that these mice have intrinsically elevated chromosome instability. These results demonstrate the potential usefulness of this assay as a screening tool for mutations causing both spontaneous and radiation-induced chromosome instability.

Mutagenesis screen to isolate chromosome instability mutations: To identify new mutations, we mutagenized male C57BL6/J (B6) mice with ENU and used them to initiate a three-generation breeding scheme to obtain third-generation (G_3) offspring that were potentially homozygous for induced mutations (see MATERIALS AND METHODS). ENU is a potent germline point mutagen that produces functional mutations at a rate of ~1/750/locus/gamete (HITOTSUMACHI *et al.* 1985). G_3 males were screened by the micronucleus assay to detect recessive mutations affecting radiation-induced and/or spontaneous micronucleus frequencies.

In Figure 3, representative distributions of spontaneous and γ-ray-induced micronucleus frequencies in 127 G_3 males are plotted. The means (with standard deviation) were 0.21 ± 0.08% and 2.35 ± 0.70% for spontaneous and γ-ray-induced micronucleus frequencies, respectively (Figure 3, A and B).

Three different screens were conducted. In the first, 422 G_3 males descended from 39 G_1 males were tested for elevated spontaneous and radiation-induced micronucleus levels. One variant appeared as an outlier, which was defined as an individual with micronucleus levels higher than three standard deviations of the mean. This variant exhibited significantly elevated levels of both

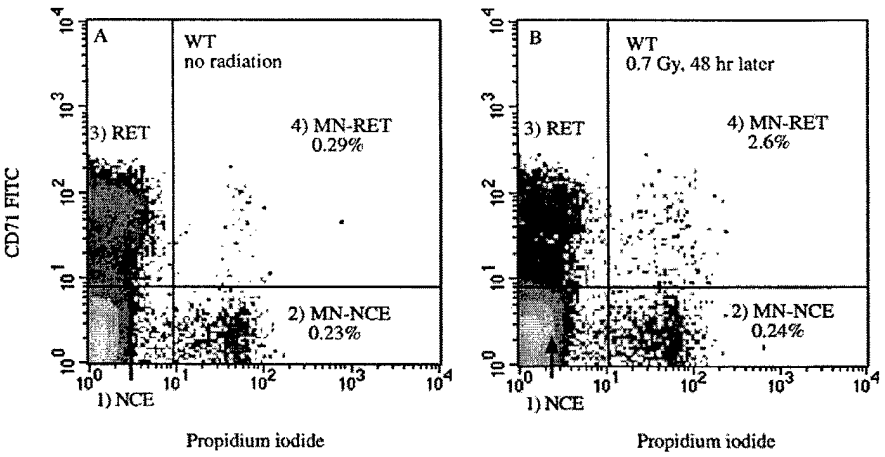

FIGURE 1.—Representative data from the flow cytometric micronucleus assay. Peripheral blood from a wild-type animal before (A) and 48 hr after (B) γ-irradiation was analyzed. CD71-positive RETs (populations 3 and 4) are separated from CD71-negative NCEs (populations 1 and 2) to enumerate radiation-induced micronuclei. MN-NCEs and MN-RETs are stained with propidium iodide and shown as populations 2 and 4, respectively.

spontaneous and radiation-induced micronucleated erythrocytes (Figure 3, A and B). Moreover, the number of RETs was decreased markedly after irradiation (to 0.26% of total erythrocytes) as seen in Figure 3C, indicating its hypersensitivity to γ-rays. This trait was determined to be recessive and exhibited Mendelian segregation. This mutation, *chaos1*, is described below.

Since a positive correlation between spontaneous and induced micronucleus levels has been reported in a number of mouse strains (SALAMONE and MAVOURNIN 1994), mice generated in the subsequent screens were tested only for spontaneous micronucleus levels. In the second screen, one potential mutation was recovered among 212 G_3 males derived from 20 G_1 males. This potential mutation is being tested to characterize radiation sensitivity and genetic heritability. The third screen involved mice produced in an ongoing region-specific mutagenesis project in our laboratory designed to detect various mutations on proximal chromosome 5 (SCHIMENTI and BUCAN 1998). Out of 336 G_3 males screened from 336 families (see MATERIALS AND METHODS), we have identified two mutations conferring higher spontaneous micronucleus levels. However, these two mutations were not linked to chromosome 5. Overall, three mutations and one potential mutation have been recovered among 970 G_3 males derived from 395 G_1 males. The results of all the screens are summarized in Table 1.

***chaos1* mutation:** Since the DNA content of micronuclei in *chaos1/chaos1* mice spans a wide range, it is likely that the micronuclei contain fragments of chromosomes, indicative of a failure to properly repair DSBs. DSBs are repaired in mammalian cells by one of two pathways: NHEJ and HR. Mice deficient in all known components of the NHEJ pathway show a SCID phenotype, due to defects in V(D)J recombination that lead to serious impairment of immune function (MULLER *et al.* 1999). Although there were no overt indications that *chaos1* mutants were immunodeficient, experiments were performed to test this possibility. Peripheral blood of *chaos1/chaos1* mice was stained with anti-CD3ε-PE and anti-Ig κ light chain-FITC antibodies to mark T- and B-cells, respectively. *chaos1/chaos1* mice had normal numbers of B- and T-cells, unlike a classic SCID profile (Figure 4A). To evaluate *chaos1* mutants for potential HR repair defects, we challenged them with mitomycin C (MMC), which causes DNA interstrand crosslinks. Since mutations in the *RAD51*-related genes *XRCC2* and *XRCC3* confer MMC hypersensitivity, it has been sug-

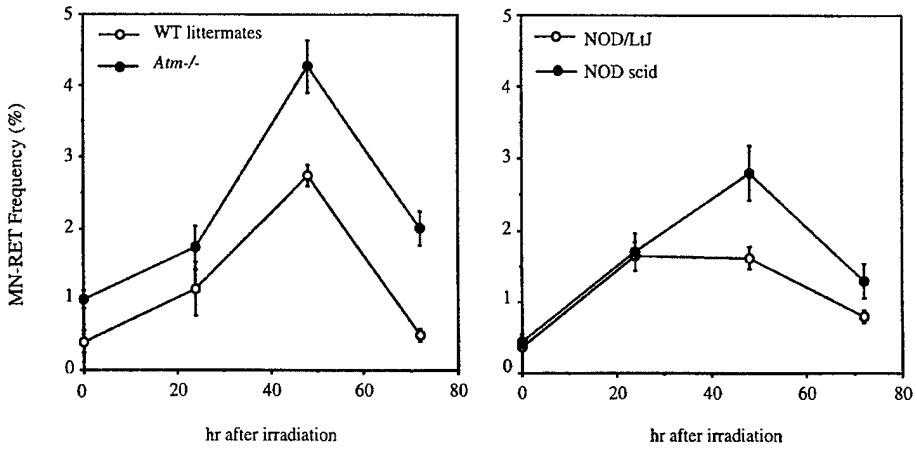

FIGURE 2.—Higher micronucleus levels in radiation-sensitive mutants. Homozygous mutants at *Atm* or *Prkdc* and their control strains (wild-type littermates for $Atm^{-/-}$ mutants and NOD/LtJ for NOD scid) were exposed to 0.7 Gy γ-ray. Peripheral blood was collected from the animals every 24 hr up to 72 hr from the time of irradiation and was analyzed by the flow cytometric micronucleus assay. Each point is shown with standard deviation. At least five animals were used per group.

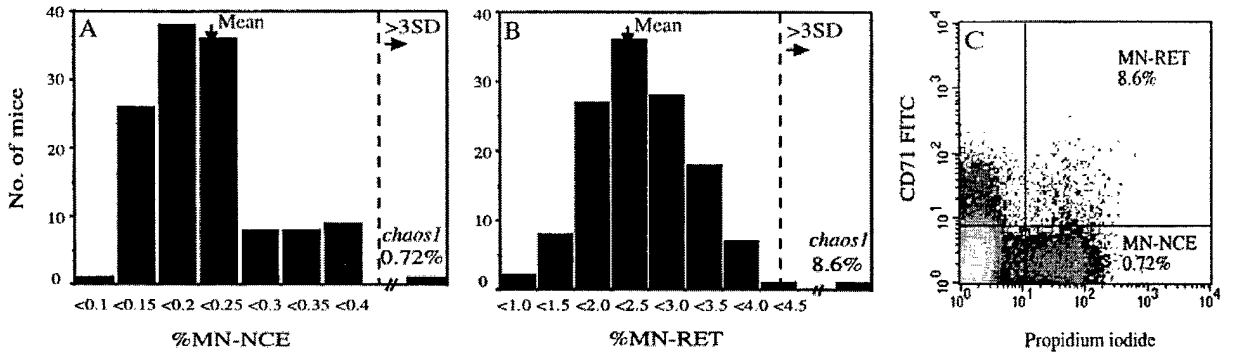

FIGURE 3.—Distribution of micronucleus frequency in NCEs and RETs in G_3 animals. *chaos1* appeared as an outlier with significantly higher spontaneous (A) and radiation-induced (B) micronucleus frequencies. Both exceed three standard deviations (3 SD). The flow plot of *chaos1* is shown in C. Two million erythrocytes were analyzed to collect 5000 RETs because of an extremely low number of RETs in this mutant after irradiation.

gested that crosslinks are repaired by the HR pathway (THACKER 1999). *chaos1/chaos1* mice had higher levels of micronuclei in response to MMC than did their wild-type littermates ($P = 0.0039$; see Figure 4B), suggesting that these mice are defective in HR repair or crosslink repair.

Aside from the phenotypes of elevated micronuclei and radiosensitivity of reticulocytes, *chaos1/chaos1* mutants are fertile and appear normal in all other respects up to 18 months of age. Radiation-induced tumorigenesis is being investigated in *chaos1/chaos1* mice rendered congenic in particular strain backgrounds. Tail fibroblasts isolated from *chaos1/chaos1* mice did not appear to be significantly sensitive to radiation compared to those from wild type (data not shown); thus this phenotype might be restricted to hematopoietic cells.

***chaos1* mapping:** We genetically mapped *chaos1* to an ~3-cM interval between *D16Mit4* and *D16Mit125* on chromosome 16 by performing genome scans of affected animals (97 meioses) produced in matings of homozygous G_3 animals to their heterozygous G_1 or G_2 parents (using microsatellite markers polymorphic between B6 and C3H). We then conducted a larger intersubspecific backcross by crossing *chaos1/chaos1* mice to *Mus castaneus* (CAST/Ei) and then backcrossing the F_1's to *chaos1* homozygotes. The resulting 1710 progeny were typed with existing and newly developed polymorphic microsatellite markers in the critical region of MMU16, and recombinants were phenotyped by the micronucleus assay. Exploiting the mouse genomic sequences in the Celera Discovery System (CDS), we localized *chaos1* to a 1.3-Mb interval between *D16Mit11* and a new marker, *D16Jcs23* (Figure 5). Information on *chaos1* mapping has been deposited in the Mouse Genome Database (accession no. J:73427).

***Polq* as a candidate gene for *chaos1*:** The *chaos1* critical region is homologous to human chromosome 3q13.31, which contains the *POLQ* gene, encoding DNA polymerase θ (SHARIEF *et al.* 1999). Among 22 genes predicted by the CDS in the *chaos1* critical region (see Figure 5), *Polq* is an attractive candidate for *chaos1*, because its protein sequence is homologous to that encoded by *Drosophila melanogaster mus308* (*mu*tagen *s*ensitivity *308*), a gene believed to be involved in interstrand crosslink repair (BOYD *et al.* 1990). *mus308* encodes a 229-kD polypeptide containing seven conserved motifs characteristic of DNA and RNA helicases in an amino-terminal domain. The carboxy-terminal domain shares similarity

TABLE 1

Summary of the MN screens

Type of screen	No. of G_3 males	No. of G_1 males	No. of mutations	Remarks
Genome wide				
Radiation-induced and spontaneous MN	422	39	1	*chaos1*
Spontaneous MN	212	20	1	Putative
Chromosome 5				
Spontaneous MN	336[a]	336	2[b]	
Total	970	395	4	

[a] G_3 animals in this screen were generated by intercrosses between G_2 males and G_2 females.
[b] These mutations are not linked to chromosome 5.

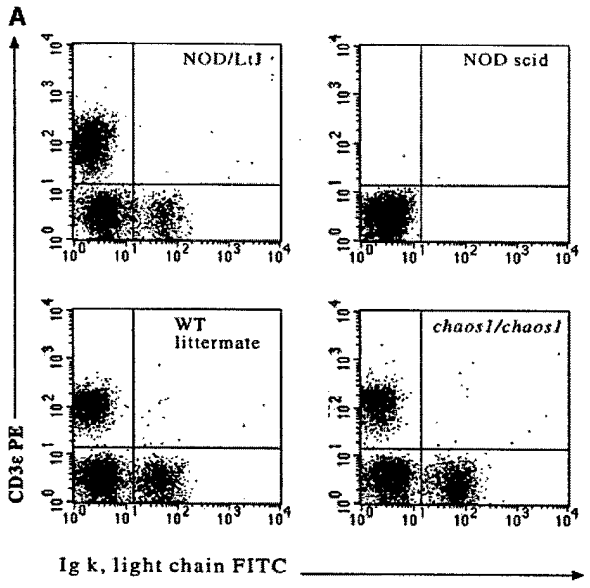

FIGURE 4.—Phenotypes of *chaos1/chaos1* mice. (A) *chaos1* mutants have normal B- and T-cell production. Peripheral blood from *chaos1/chaos1* mice and their wild-type littermate was stained with anti-Ig κ light chain and anti-CD3ε-PE to label B- and T-cells, respectively. NOD/LtJ and NOD scid mice were used as positive and negative controls, respectively. (B) Mitomycin C sensitivity of *chaos1* mutants revealed by the micronucleus assay. *chaos1* mutants and their wild-type littermates were given 1 mg/kg of MMC. Peripheral blood was sampled every 24 hr and analyzed for MMC-induced micronuclei in RETs. At least five animals were used per group and data are shown with standard deviations.

with the polymerase domain of prokaryotic DNA polymerase I-like enzymes (HARRIS *et al.* 1996). The presence of two such domains in a protein is unique.

The CDS predicted the existence of a gene sharing homology with human *POLQ* in the *chaos1* critical region. RT-PCR was performed with primers designed to the predicted mouse gene, yielding partial cDNAs from testis of B6 mice. The overlapping partial cDNAs were used to identify an open reading frame of 7635 nucleotides (Figure 6A), which encodes a polypeptide of 2544 amino acids (GenBank accession no. AY074936). As predicted, this polypeptide contains helicase and DNA polymerase motifs and it has 68% amino acid identity to human POLQ containing 2724 amino acids (AY032677; Clustal W 1.4 alignment).

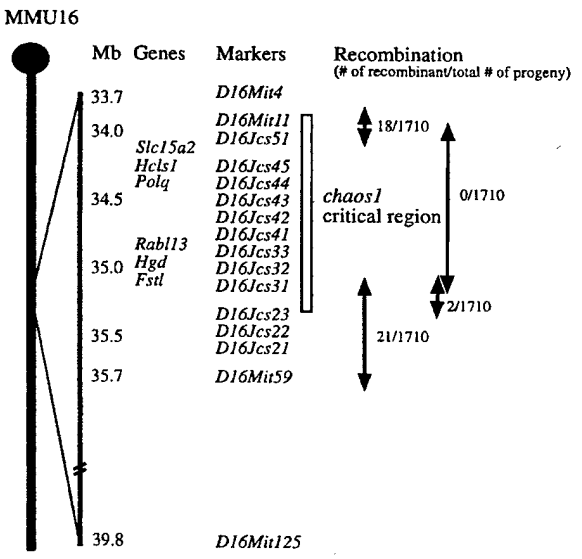

FIGURE 5.—The *chaos1* critical region. Physical location of all known genes and microsatellite markers are shown, using data from the Celera Discovery System. *D16Jcs* markers, which are polymorphic between B6 and CAST/Ei, were designed for this study. Data from the intersubspecific mapping backcross between *chaos1* and CAST/Ei, which were used to determine the *chaos1* critical region, are shown. Twenty-two genes predicted by the CDS are in this region.

The Celera mouse genome sequence was used to reveal that a total of 30 exons comprise this *Polq* cDNA (Figure 6A). Similarly, exploiting the Celera human genome sequence, 31 exons were found for *POLQ*. As shown in Figure 6B, a shorter transcript, which skips exons 6–10, was also found in mouse testis, giving rise to a predicted polypeptide of 2265 amino acids (AY147862). Moreover, each of the *Polq* transcripts has a longer isoform containing one extra exon (exon 4); however, the presence of this exon creates a stop codon (AY147863, AY147864). A Riken mouse cDNA from neonatal thymus has full-length exons 2 and 5, also containing a stop codon (AK020790). Collectively, 31 *Polq* exons were found; however, the roles of these various transcripts remain to be elucidated.

There was no indication of differences in transcript size or expression levels in mutant RNA compared to that from wild-type B6 mice (data not shown). Nevertheless, a single T → C base substitution was identified at residue 5794 in the coding region (exon 19) of the *chaos1*

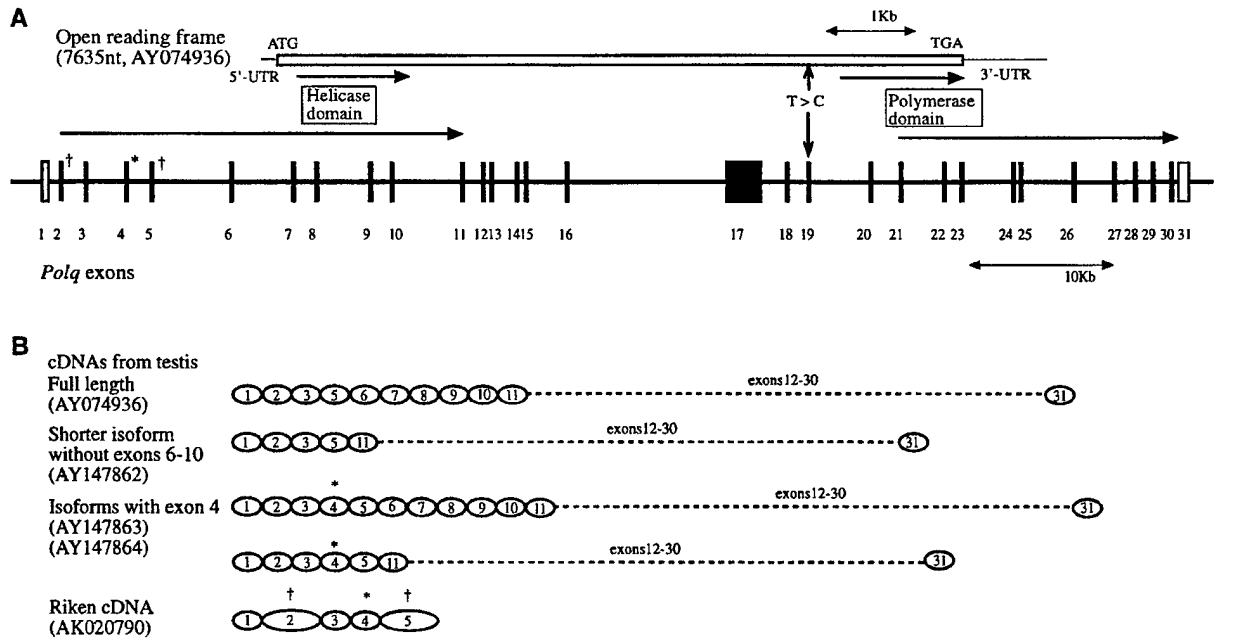

FIGURE 6.—Structure of the *Polq* gene and transcripts. (A) An open reading frame flanked by 5′- and 3′-untranslated regions (UTR) in *Polq* cDNA is shown to scale (above) with the start codon and stop codon. The Celera mouse genome sequence was used to reveal that a total of 30 exons encode this *Polq* cDNA (AY074936). Exons (small rectangles) and introns in the *Polq* gene are shown to scale (below). Exons 1 and 31 (small unfilled rectangles) contain the 5′- and 3′-UTRs, respectively. The T → C transition found in *chaos1* mutant is indicated. The regions of helicase and DNA polymerase homology and the corresponding exons are also indicated as arrows. (B) Schematic illustration of exons comprising the different *Polq* transcripts. A shorter transcript that skips exons 6–10 was also identified (AY147862). (*) Longer isoforms containing one extra exon (exon 4) were also identified; however, the presence of this exon creates a stop codon (AY147863, AY147864). (†) Full-length exons 2 and 5 were found in a Riken mouse cDNA from neonatal thymus (AK020790), whereas *Polq* cDNAs from testis contain only part of exons 2 and 5, because of alternative splicing of these exons. Collectively, 31 *Polq* exons were found.

mutant allele (Figure 6A), which is not present in B6 cDNA. This mutation gives rise to a serine-to-proline change at residue 1932.

DISCUSSION

To our knowledge, this is the first successful phenotype-driven screen for chromosome instability mutants in mice. The micronucleus assay adapted from the method developed by DERTINGER *et al.* (1996) was highly sensitive and readily implemented as a high-throughput screen for mutagenized mice. The dose of γ-rays used in this screen had little effect on the reproductive ability of the G_3 males, which were subsequently used for mapping studies or maintenance of the mutation. Only males were screened in this study due to logistical factors associated with the mutagenesis program from which the mice were derived. However, the spontaneous micronucleus frequencies tended to be lower in females than in males.

Importantly, the high reproducibility of the assay (DERTINGER *et al.* 2000; TOROUS *et al.* 2001) allowed accurate phenotyping of mice in the mapping crosses, which is critical for positional cloning. In the case of *chaos1* phenotyping, there was no need to irradiate mice, because the mutants were easily identified by high spontaneous micronucleus levels. Actually, we find it more practical and feasible to perform screens only for spontaneously elevated micronucleus levels. Potential mutants isolated can be characterized later as to sensitivity to radiation or other agents. Moreover, micronuclei can be isolated by flow sorting or microdissection for further analysis (NUSSE *et al.* 1996; PEACE *et al.* 1999) to characterize phenotypes of identified mutants.

The presence of a mutated *Polq* allele in *chaos1* mice makes this gene a strong candidate for *chaos1*. The identified T → C transition is one of the two most frequent classes of ENU-induced mutations in the mouse germline (MARKER *et al.* 1997; JUSTICE *et al.* 1999). This mutation causes a drastic amino acid change in POLQ from serine to proline, which may alter the secondary structure of the molecule. However, since the mutation is not located in either the helicase or the polymerase domains of the predicted protein (the two regions of the protein about which we can make informed speculation as to key enzymatic activity), it is difficult to draw a conclusion about the functional importance of this

particular amino acid residue or to determine if the mutation actually compromises protein function. To gain some insight into the functional importance of this amino acid residue, we compared the mouse POLQ sequence to those of other organisms. Homologs of *mus308* have been reported in *Caenorhabditis elegans*, *Arabidopsis thaliana* (Harris *et al.* 1996; Marini and Wood 2002), and humans (Sharief *et al.* 1999), but not yeast. By BLAST searching databases, we also found a presumed ortholog in *Anopheles gambiae* (mosquitos; accession no. EAA04696). The serine is conserved in human and mosquito. It exists as alanine in Drosophila (L76559) and asparagine in Arabidopsis (CAA18591), both of which are semiconservative differences. The region containing this residue in *C. elegans* (AAB93325) is too divergent to align with other *mus308* homologs.

Additional support for *Polq* as a candidate for *chaos1* is the similarity in phenotypes of *chaos1* mutants to flies containing mutations in *mus308*, a *Polq* homolog. Drosophila *mus308* encodes a unique protein with helicase and prokaryotic DNA polymerase I-like motifs in a single polypeptide (Harris *et al.* 1996). *mus308* mutants were identified as strains hypersensitive to nitrogen mustard, a crosslinking agent (Boyd *et al.* 1981), but not to a monofunctional alkylating agent, methyl methanesulfonate (Boyd *et al.* 1990), suggesting that *mus308* is specifically involved in crosslink repair. However, it has been reported that *mus308* might be also involved in postreplicational repair (Aguirrezabalaga *et al.* 1995; Tosal *et al.* 2000). Homozygous *mus308* flies showed elevated embryonic mortality associated with chromosome instability and a mutator phenotype in response to certain mutagens (Leonhardt *et al.* 1993).

Recently, human POLQ was purified as a high-fidelity DNA polymerase with the ability to bypass DNA lesions (Maga *et al.* 2002). This is quite unique among recently discovered DNA polymerases, most of which are error prone (Goodman and Tippin 2000). However, the purified POLQ did not show detectable helicase activity (Maga *et al.* 2002). New helicase genes, *HEL308* and *Hel308*, which are homologous to the helicase motif of *mus308*, have been identified in humans and mice (Marini and Wood 2002). Purified human HEL308 exhibited a DNA helicase activity (Marini and Wood 2002). The existence of these paralogs may reflect redundancy in mammalian crosslink repair in which at least two pathways have been found: recombination-dependent and recombination-independent error-prone pathways (McHugh *et al.* 2001; Wang *et al.* 2001). It remains to be elucidated how exactly these proteins function to repair crosslinks. If *chaos1* is truly a *Polq* mutation, the *chaos1* mutant may fill a unique niche that would allow *in vivo* investigation of crosslink repair in mammals.

Despite the higher micronucleus levels, *chaos1/chaos1* mutants showed no apparent abnormalities up to 18 months of age. This may not be surprising, since mouse models for Fanconi anemia, which have defects in crosslink repair, do not show a predisposition to cancer (Chen *et al.* 1996; Cheng *et al.* 2000; Yang *et al.* 2001). It has also been reported that *Xpa* or *Xpc* knockouts, deficient in nucleotide excision repair, rarely developed tumors without carcinogen treatment (Wijnhoven *et al.* 2000; van Kreijl *et al.* 2001), although $Xpc^{-/-}$ mice had a higher spontaneous mutation rate at the *Hprt* locus. In general, genome instability itself may not be sufficient to cause cancer. Other events, such as loss of cell-cycle checkpoints, could be more critical. Nevertheless, chromosome instability may facilitate the occurrence of these critical events. Indeed, introduction of a *Trp53* null allele significantly enhanced mammary tumor formation in the *Brca1* conditional mutant mice; otherwise tumorigenesis occurred after long latency and at a low frequency (Xu *et al.* 1999; Deng and Scott 2000). We have also observed a synergistic increase in genome instability and growth retardation in mice doubly mutant for *Atm* and *chaos1* (N. Shima and J. Schimenti, unpublished data).

The data presented here demonstrate the efficacy of the micronucleus screen for detecting new chromosome instability mutants and subsequently mapping them in a robust way. With this screen, it is also possible that hypomorphic alleles of important DSB repair genes such as *Rad51* paralogs, whose complete inactivation causes embryonic lethality, may be detected (Thompson and Schild 1999). The genes responsible for elevated micronuclei might be involved not only in DNA repair, but also in processes such as mitotic-spindle checkpoints, defects of which could lead to aneuploidy, the most frequent genetic abnormality observed in cancer cells (Lengauer *et al.* 1998). While it is still controversial that genome instability always leads to carcinogenesis (Marx 2002), elevated micronucleus levels could be used as a surrogate phenotype that predicts cancer predisposition at an early age. In some cases, higher micronucleus levels in peripheral blood of humans have been linked with increased cancer risk (Doneda *et al.* 1995; Scott *et al.* 1999). Development of such a surrogate phenotype would enable the screening and mapping of recessive mutations causing cancers without aging mice to the point where late-onset cancers develop.

In conclusion, the flow cytometric screen for elevated micronuclei has proven to be a useful approach to identifying mutations in novel genes that cause genome instability as a consequence of DSB repair defects. The incorporation of these screens into major mutagenesis efforts may yield new and hitherto unknown genes that contribute to cancer and concomitantly may yield the cognate mutant mouse models.

We thank Leonard Shultz, Susan Ackerman, and Jeremy Ward for critical reading of the manuscript and helpful comments. This work is supported by National Institutes of Health grants GM-45415 and HD-35984 to J.S. N.S. is supported by a postdoctoral fellowship from the Breast Cancer Research Program, Department of Defense (DAMD 17-01-1-0277).

LITERATURE CITED

AGUIRREZABALAGA, I., L. M. SIERRA and M. A. COMENDADOR, 1995 The hypermutability conferred by the mus308 mutation of Drosophila is not specific for cross-linking agents. Mutat. Res. **336:** 243–250.

BOYD, J. B., M. D. GOLINO, K. E. SHAW, C. J. OSGOOD and M. M. GREEN, 1981 Third-chromosome mutagen-sensitive mutants of *Drosophila melanogaster.* Genetics **97:** 607–623.

BOYD, J. B., K. SAKAGUCHI and P. V. HARRIS, 1990 mus308 mutants of Drosophila exhibit hypersensitivity to DNA cross-linking agents and are defective in a deoxyribonuclease. Genetics **125:** 813–819.

CHEN, M., D. J. TOMKINS, W. AUERBACH, C. MCKERLIE, H. YOUSSOUFIAN *et al.*, 1996 Inactivation of Fac in mice produces inducible chromosomal instability and reduced fertility reminiscent of Fanconi anaemia. Nat. Genet. **12:** 448–451.

CHENG, N. C., H. J. VAN DE VRUGT, M. A. VAN DER VALK, A. B. OOSTRA, P. KRIMPENFORT *et al.*, 2000 Mice with a targeted disruption of the Fanconi anemia homolog Fanca. Hum. Mol. Genet. **9:** 1805–1811.

DENG, C. X., and F. SCOTT, 2000 Role of the tumor suppressor gene Brca1 in genetic stability and mammary gland tumor formation. Oncogene **19:** 1059–1064.

DERTINGER, S. D., D. K. TOROUS and K. R. TOMETSKO, 1996 Simple and reliable enumeration of micronucleated reticulocytes with a single-laser flow cytometer. Mutat. Res. **371:** 283–292.

DERTINGER, S. D., D. K. TOROUS, N. E. HALL, C. R. TOMETSKO and T. A. GASIEWICZ, 2000 Malaria-infected erythrocytes serve as biological standards to ensure reliable and consistent scoring of micronucleated erythrocytes by flow cytometry. Mutat. Res. **464:** 195–200.

DIGWEED, M., A. REIS and K. SPERLING, 1999 Nijmegen breakage syndrome: consequences of defective DNA double strand break repair. Bioessays **21:** 649–656.

DONEDA, L., G. BASILISCO, P. BIANCHI and L. LARIZZA, 1995 High spontaneous chromosomal damage in lymphocytes from patients with hereditary megaduodenum. Mutat. Res. **348:** 33–36.

FRIEDBERG, E. C., G. C. WALKER and W. SIEDE, 1995 *DNA Repair and Mutagenesis.* ASM Press, Washington, DC.

GOODMAN, M. F., and B. TIPPIN, 2000 The expanding polymerase universe. Nat. Rev. Mol. Cell Biol. **1:** 101–109.

HARRIS, P. V., O. M. MAZINA, E. A. LEONHARDT, R. B. CASE, J. B. BOYD *et al.*, 1996 Molecular cloning of Drosophila mus308, a gene involved in DNA cross-link repair with homology to prokaryotic DNA polymerase I genes. Mol. Cell. Biol. **16:** 5764–5771.

HAYASHI, M., T. MORITA, Y. KODAMA, T. SOFUNI and M. ISHIDATE, JR., 1990 The micronucleus assay with mouse peripheral blood reticulocytes using acridine orange-coated slides. Mutat. Res. **245:** 245–249.

HEDDLE, J. A., 1973 A rapid in vivo test for chromosomal damage. Mutat. Res. **18:** 187–190.

HENDRICKSON, E. A., 1997 Cell-cycle regulation of mammalian DNA double-strand-break repair. Am. J. Hum. Genet. **61:** 795–800.

HITOTSUMACHI, S., D. A. CARPENTER and W. L. RUSSELL, 1985 Dose-repetition increases the mutagenic effectiveness of N-ethyl-N-nitrosourea in mouse spermatogonia. Proc. Natl. Acad. Sci. USA **82:** 6619–6621.

HRABE DE ANGELIS, M. H., H. FLASWINKEL, H. FUCHS, B. RATHKOLB, D. SOEWARTO *et al.*, 2000 Genome-wide, large-scale production of mutant mice by ENU mutagenesis. Nat. Genet. **25:** 444–447.

JONES, N. J., R. COX and J. THACKER, 1987 Isolation and cross-sensitivity of X-ray-sensitive mutants of V79-4 hamster cells. Mutat. Res. **183:** 279–286.

JONES, N. J., R. COX and J. THACKER, 1988 Six complementation groups for ionising-radiation sensitivity in Chinese hamster cells. Mutat. Res. **193:** 139–144.

JUSTICE, M. J., 1999 Mutagenesis of the mouse germline, pp. 185–215 in *Mouse Genetics and Transgenics: A Practical Approach,* edited by I. JACKSON and C. ABBOTT. Oxford University Press, Oxford.

JUSTICE, M. J., J. K. NOVEROSKE, J. S. WEBER, B. ZHENG and A. BRADLEY, 1999 Mouse ENU mutagenesis. Hum. Mol. Genet. **8:** 1955–1963.

KARRAN, P., 2000 DNA double strand break repair in mammalian cells. Curr. Opin. Genet. Dev. **10:** 144–150.

KHANNA, K. K., and S. P. JACKSON, 2001 DNA double-strand breaks: signaling, repair and the cancer connection. Nat. Genet. **27:** 247–254.

KRAAKMAN-VAN DER ZWET, M., W. J. OVERKAMP, R. E. VAN LANGE, J. ESSERS, A. VAN DUIJN-GOEDHART *et al.*, 2002 Brca2 (XRCC11) deficiency results in radioresistant DNA synthesis and a higher frequency of spontaneous deletions. Mol. Cell. Biol. **22:** 669–679.

LENGAUER, C., K. W. KINZLER and B. VOGELSTEIN, 1998 Genetic instabilities in human cancers. Nature **396:** 643–649.

LEONHARDT, E. A., D. S. HENDERSON, J. E. RINEHART and J. B. BOYD, 1993 Characterization of the mus308 gene in *Drosophila melanogaster.* Genetics **133:** 87–96.

MAGA, G., I. SHEVELEV, K. RAMADAN, S. SPADARI and U. HUBSCHER, 2002 DNA polymerase theta purified from human cells is a high-fidelity enzyme. J. Mol. Biol. **319:** 359–369.

MARINI, F., and R. D. WOOD, 2002 A human DNA helicase homologous to the DNA cross-link sensitivity protein Mus308. J. Biol. Chem. **277:** 8716–8723.

MARKER, P. C., K. SEUNG, A. E. BLAND, L. B. RUSSELL and D. M. KINGSLEY, 1997 Spectrum of *Bmp5* mutations from germline mutagenesis experiments in mice. Genetics **145:** 435–443.

MARX, J., 2002 Debate surges over the origins of genomic defects in cancer. Science **297:** 544–546.

MCHUGH, P. J., V. J. SPANSWICK and J. A. HARTLEY, 2001 Repair of DNA interstrand crosslinks: molecular mechanisms and clinical relevance. Lancet Oncol. **2:** 483–490.

MEYN, M. S., 1999 Ataxia-telangiectasia, cancer and the pathobiology of the ATM gene. Clin. Genet. **55:** 289–304.

MORITA, T., N. ASANO, T. AWOGI, Y. F. SASAKI, S. SATO *et al.*, 1997 Evaluation of the rodent micronucleus assay in the screening of IARC carcinogens (groups 1, 2A and 2B): the summary report of the 6th collaborative study by CSGMT/JEMS MMS. Collaborative Study of the Micronucleus Group Test. Mammalian Mutagenicity Study Group. Mutat. Res. **389:** 3–122.

MULLER, C., P. CALSOU, P. FRIT and B. SALLES, 1999 Regulation of the DNA-dependent protein kinase (DNA-PK) activity in eukaryotic cells. Biochimie **81:** 117–125.

NUSSE, M., B. M. MILLER, S. VIAGGI and J. GRAWE, 1996 Analysis of the DNA content distribution of micronuclei using flow sorting and fluorescent in situ hybridization with a centromeric DNA probe. Mutagenesis **11:** 405–413.

PEACE, B. E., G. LIVINGSTON, E. B. SILBERSTEIN and J. C. LOPER, 1999 A case of elevated spontaneous micronucleus frequency derived from chromosome 2. Mutat. Res. **430:** 109–119.

SALAMONE, M. F., and K. H. MAVOURNIN, 1994 Bone marrow micronucleus assay: a review of the mouse stocks used and their published mean spontaneous micronucleus frequencies. Environ. Mol. Mutagen. **23:** 239–273.

SCHIMENTI, J., and M. BUCAN, 1998 Functional genomics in the mouse: phenotype-based mutagenesis screens. Genome Res. **8:** 698–710.

SCOTT, D., J. B. BARBER, A. R. SPREADBOROUGH, W. BURRILL and S. A. ROBERTS, 1999 Increased chromosomal radiosensitivity in breast cancer patients: a comparison of two assays. Int. J. Radiat. Biol. **75:** 1–10.

SERKE, S., and D. HUHN, 1992 Identification of CD71 (transferrin receptor) expressing erythrocytes by multiparameter-flow-cytometry (MP-FCM): correlation to the quantitation of reticulocytes as determined by conventional microscopy and by MP-FCM using a RNA-staining dye. Br. J. Haematol. **81:** 432–439.

SHARIEF, F. S., P. J. VOJTA, P. A. ROPP and W. C. COPELAND, 1999 Cloning and chromosomal mapping of the human DNA polymerase theta (POLQ), the eighth human DNA polymerase. Genomics **59:** 90–96.

SHEN, S. X., Z. WEAVER, X. XU, C. LI, M. WEINSTEIN *et al.*, 1998 A targeted disruption of the murine Brca1 gene causes gamma-irradiation hypersensitivity and genetic instability. Oncogene **17:** 3115–3124.

THACKER, J., 1999 The role of homologous recombination processes in the repair of severe forms of DNA damage in mammalian cells. Biochimie **81:** 77–85.

THOMPSON, L. H., and D. SCHILD, 1999 The contribution of homologous recombination in preserving genome integrity in mammalian cells. Biochimie **81:** 87–105.

THOMPSON, L. H., and D. SCHILD, 2001 Homologous recombina-

tional repair of DNA ensures mammalian chromosome stability. Mutat. Res. **477:** 131–153.

THOMPSON, L. H., K. W. BROOKMAN, L. E. DILLEHAY, A. V. CARRANO, J. A. MAZRIMAS *et al.*, 1982 A CHO-cell strain having hypersensitivity to mutagens, a defect in DNA strand-break repair, and an extraordinary baseline frequency of sister-chromatid exchange. Mutat. Res. **95:** 427–440.

TOROUS, D. K., N. E. HALL, S. D. DERTINGER, M. S. DIEHL, A. H. ILLI-LOVE *et al.*, 2001 Flow cytometric enumeration of micronucleated reticulocytes: high transferability among 14 laboratories. Environ. Mol. Mutagen. **38:** 59–68.

TOSAL, L., M. A. COMENDADOR and L. M. SIERRA, 2000 The mus308 locus of Drosophila melanogaster is implicated in the bypass of ENU-induced O-alkylpyrimidine adducts. Mol. Gen. Genet. **263:** 144–151.

TRUETT, G. E., P. HEEGER, R. L. MYNATT, A. A. TRUETT, J. A. WALKER *et al.*, 2000 Preparation of PCR-quality mouse genomic DNA with hot sodium hydroxide and tris (HotSHOT). Biotechniques **29:** 52–54.

TUTT, A., A. GABRIEL, D. BERTWISTLE, F. CONNOR, H. PATERSON *et al.*, 1999 Absence of Brca2 causes genome instability by chromosome breakage and loss associated with centrosome amplification. Curr. Biol. **9:** 1107–1110.

VAN BRABANT, A. J., R. STAN and N. A. ELLIS, 2000 DNA helicases, genomic instability, and human genetic disease. Annu. Rev. Genomics Hum. Genet. **1:** 409–459.

VAN GENT, D. C., J. H. HOEIJMAKERS and R. KANAAR, 2001 Chromosomal stability and the DNA double-stranded break connection. Nat. Rev. Genet. **2:** 196–206.

VAN KREIJL, C. F., P. A. MCANULTY, R. B. BEEMS, A. VYNCKIER, H. VAN STEEG *et al.*, 2001 Xpa and Xpa/p53+/− knockout mice: overview of available data. Toxicol. Pathol. **29:** 117–127.

VENKITARAMAN, A. R., 2002 Cancer susceptibility and the functions of BRCA1 and BRCA2. Cell **108:** 171–182.

WANG, X., C. A. PETERSON, H. ZHENG, R. S. NAIRN, R. J. LEGERSKI *et al.*, 2001 Involvement of nucleotide excision repair in a recombination-independent and error-prone pathway of DNA interstrand cross-link repair. Mol. Cell. Biol. **21:** 713–720.

WIJNHOVEN, S. W., H. J. KOOL, L. H. MULLENDERS, A. A. VAN ZEELAND, E. C. FRIEDBERG *et al.*, 2000 Age-dependent spontaneous mutagenesis in Xpc mice defective in nucleotide excision repair. Oncogene **19:** 5034–5037.

XU, X., K. U. WAGNER, D. LARSON, Z. WEAVER, C. LI *et al.*, 1999 Conditional mutation of Brca1 in mammary epithelial cells results in blunted ductal morphogenesis and tumour formation. Nat. Genet. **22:** 37–43.

YANG, Y., Y. KUANG, R. M. DE OCA, T. HAYS, L. MOREAU *et al.*, 2001 Targeted disruption of the murine Fanconi anemia gene, Fancg/Xrcc9. Blood **98:** 3435–3440.

ZDZIENICKA, M. Z., 1999 Mammalian X-ray-sensitive mutants which are defective in non-homologous (illegitimate) DNA double-strand break repair. Biochimie **81:** 107–116.

Communicating editor: D. KINGSLEY